FAST NEUTRON CAPTURE ON Ir ISOTOPES

By M. Herman, A. Marcinkowski

Institute for Nuclear Studies, Warsaw*

and G. Reffo

National Committee of Nuclear and Alternative Energies, Bologna, Italy

(Received May 23, 1984)

Neutron capture cross sections on ^{191,193}Ir were measured by the activation technique. The results are discussed in terms of the compound nucleus formation mechanism.

PACS numbers: 25.40.Lw

1. Introduction

Capture cross section measurements using activation technique in the MeV region are complicated mainly due to the accompanying parasitic neutron producing reactions. Since the capture cross section increases rapidly with decreasing neutron energy even small contaminations by low energy neutrons, scattered in the target backing or in the sample itself, may lead to serious disturbance of the measurement. These effects have been studied systematically in Refs. [1, 2] and the resulting precautions have been followed in the present measurement of the capture cross sections on iridium isotopes in the neutron energy range from 0.3 to 1.3 MeV. The present measurement has been undertaken in order to prove the ability of the compound nucleus concept to describe such cross sections with enough accuracy. It has been shown earlier that the simpler mechanisms like direct and semidirect or collective capture do not play a significant role at such low energies [3, 4]. On the other hand the new statistical approach [5] to the evaluation of the width fluctuations allows one to search enhancement effects [6], which however disappear for heavy nuclei, where large number of channels is involved.

2. Experimental procedure

Natural, high purity, metallic Ir and enriched ^{191}Ir (98.17%), loaned from the International Atomic Energy Agency, has been irradiated with neutrons from the ^{3}H(p,n)^{3}He reaction. Tritium absorbed in a thin transmissive Ti layer, evaporated on copper backing,

* Address: Instytut Problemów Jądrowych, Hoża 69, 00-681 Warszawa, Poland.

was bombarded with protons accelerated in a 3 MeV Van de Graaff accelerator of the Institute for Nuclear Studies in Warsaw. For monitoring the fluctuations of the neutron flux during the irradiation the pulses from a long counter have been detected in a multiscaler mode. The neutron energy was selected by a proper choice of the neutron emission angle and the energy of the protons. The neutron energy spread was evaluated from the effective energy distribution of neutrons incident on the samples, which have been calculated with aid of a Monte Carlo code LOS [7], with account for the activation geometry, for the dependence of neutron energy upon emission angle and for proton energy loss in the titanium-tritium layer of the target.

In order to avoid non-negligible contaminations by secondary neutrons, due to inelastic scattering in the activated sample material, the iridium samples were thin sheets of 675 mg/cm^2 thickness. The samples have been contained in a holder made of aluminium, which has a high 842 keV inelastic scattering threshold. The tritium target backing was 0.5 mm. A possible effect of the low energy background neutrons was controlled by simultaneous measurements of the ratio of yields of two monitoring reactions, the ^{115}In(n, γ)^{116m}In and the ^{115}In(n, n')^{115m}In reaction. The excitation curves of these reactions have opposite slopes and the cross section ratio is a sensitive measure of admixtures of low energy background neutrons. No significant effect was observed. In order to avoid contributions from neutrons, which have been thermalized in the walls of the target room all samples were encapsulated in cadmium containers during the irradiation.

Irradiations lasted usually three half-lives. The yields of the investigated reactions have been determined by following the decay of the induced γ-ray activities with use of a 40 ccm Ge(Li) spectrometer. The spectrometer was equipped with standard ORTEC electronics and a ND-4420 analysing system, which allowed programming and automatic timing of the measurement. The relative efficiency curve for the Ge(Li) crystal was determined with use of radioactive sources ^{169}Yb and ^{226}Ra. The γ-ray spectra were recorded about twice per half-life for each sample. The decay data have been analysed using a least squares fitting code ZORBUM [8], with the half-lives assumed (see Table I). The investigated γ-ray yields were referred to the yield of the 417 keV γ-rays following the decay of ^{116m}In from the ^{115}In(n, γ)^{116m}In standard reaction of known cross section [9]. In Table I the decay characteristics including the energies of the measured γ-rays are gathered. In case of the residual nucleus ^{192}Ir the cumulative decay of its ground state, with half-life 74 d has been followed. The interference caused by the two isomeric states in ^{192}Ir allows one to determine by activation a cross section, which equals $\sigma_g + 1.000014\sigma_{m1} - 0.00055\sigma_{m2}$.

TABLE I

Decay characteristics of the investigated residual nuclei

Reaction	E_γ (keV)	$T_{1/2}$	Branching ratio	Conversion coefficient
^{191}Ir(n, γ)^{192g}Ir	308+316	74 d	0.342, 0.945	0.092, 0.078
	468	74 d	0.514	0.0274
^{193}Ir(n, γ)^{194}Ir	328	19.2 h	0.14	0.0764

The measured cross sections were corrected for the attenuation of γ-rays in the sample and container materials, and for summing of pulses in the Ge(Li) crystal due to cascades of γ-transitions. In the latter correction the angular distributions of emitted γ-rays have been assumed isotropic. The resulting multiplicative correction factor κ reads,

$$\kappa^{-1} = \left[\prod_{i=1}^{m-1}\left(1-\frac{\eta_i}{1+\alpha_i}a_i\right)\right]\left[\prod_{i=m+1}^{N}\left(1-\frac{\eta_i}{1+\alpha_i}a_i b_i\right)\right], \quad (1)$$

and applies to cross section determined via measuring a transition m, which is in cascade with $m-1$ subsequent preceding γ-transitions and $N-m$ subsequent following transitions. a_i, b_i, α_i and η_i denote the attenuation in the sample material, the branching ratio, the conversion coefficient and the detection efficiency, respectively. Formula (1) can be easily generalized to include parallel transitions. The decay of ^{192}Ir leads to cascades of γ-rays in ^{192}Pt with multiplicity between 2 and 3. The corresponding correction compensating the removal of pulses from the photopeak amounts up to 13%.

3. *Results*

The measured neutron capture cross sections are compiled in Table II and in Fig. 1. The errors shown contain both statistical and systematic errors. The latter ones account for the uncertainty in: a) detection efficiency, amounting to 1.5%, b) determination of

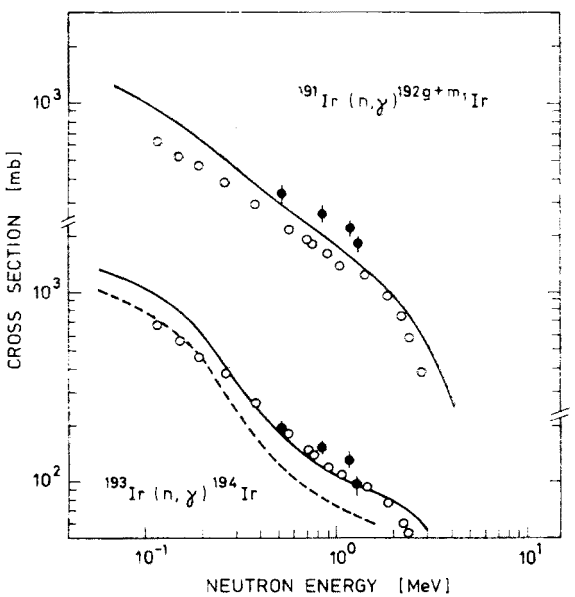

Fig. 1. Comparison between model calculations and the experimental cross sections for the neutron capture on ^{191}Ir and ^{193}Ir. The filled circles are present results, the open ones are from Ref. [10]. For description of calculations see text

TABLE II

Cross sections for neutron capture

E_n MeV	$^{191}Ir(n,\gamma)^{192g+m1}Ir$ mb	$^{193}Ir(n,\gamma)^{194}Ir$ mb	Reference cross section mb
0.53 ± 0.14	333 ± 36[a]	187 ± 20	180
0.86 ± 0.21	266 ± 29	151 ± 16	200
1.20 ± 0.15	225 ± 24	129 ± 14	176
1.31 ± 0.07	180 ± 19	91 ± 14	170

[a] measured $\sigma_g - 1.000014\sigma_{m1} - 0.00055\sigma_{m2}$.

the γ-ray attenuation in the sample material up to 5%, c) integration of the pulse height spectrum, up to 3%, d) determination of the correction for summing of cascading γ-rays in the Ge(Li) crystal, up to 5%, and e) of the cross section of the monitoring reaction $^{115}In(n,\gamma)^{116m}In$, which reaches 7% [9].

Fast neutron capture has been studied earlier by Lindner et al. [10] on both iridium isotopes and by Tolstikov et al. [11] on ^{193}Ir. The two data sets for ^{193}Ir are consistent and agree with the results of the present experiment. In case of ^{191}Ir our cross sections are higher by about 30%.

4. Theoretical calculations and discussion

The calculations of the capture cross sections have been performed along the formalism proposed by Tepel et al. [12]. It has been shown that the compound nucleus cross section $\sigma^{CN}_{a,b}$ factorizes

$$\sigma^{CN}_{a,b} = \pi\lambda_a^2 \sum_{J^\pi=0}^{\infty} \sum_{S=|I_i-s|}^{I_i+s} \sum_{l=|J-S|}^{J+S} \frac{2J+1}{2(2I+1)} V_a$$

$$\times \sum_{S'=|I_f-s|}^{I_f+s} \sum_{l'=|J-S'|}^{J+S'} \frac{V_b \varrho_b(U, I_f)}{\int dU \sum_c \sum_{I_f'} \sum_{S_c'} \sum_{l_c'} V_c \varrho_c(U, I_f')} [1+\delta_{ab}(W_a-1)], \qquad (2)$$

with the angular momentum effects included. Here S, l, J are the channel spin, orbital angular momentum and compound nucleus spin, respectively. For the outgoing channel the same but primed notation holds. I_i and I_f are the target and residual nucleus spins and s denotes the nucleon spin value. The summation over c accounts for all the open channels, $c \equiv (c', S'', l'')$ with c' denoting the kind of particle emitted.

The unitarity of the S-matrix yields the relation between V_a and the optical model transmission coefficients T_a

$$T_a = V_a + V_a^2 \Big(\sum_c V_c\Big)^{-1} (W_a - 1). \qquad (3)$$

The width fluctuation effects, which influence significantly the cross sections provided a low number of reaction channels is open [13], demonstrate themselves in an enhancement of the elastic scattering by a factor W_a, which varies between the limits 2 and 3 for strong and weak absorption, respectively. The elastic enhancement W_a has been related to the transmission coefficients T_c by generating numerically the statistical S-matrix [14],

$$W_a = 1 + \frac{2}{1+T_a^2} + (87 \pm 5)\left(\frac{T_a - \overline{T}}{\sum_c T_c}\right)^2 \left(\frac{T_a}{\sum_c T_c}\right)^5, \tag{4}$$

with

$$\alpha = 4\frac{\overline{T}}{\sum_c T_c}\left(1 + \frac{T_a}{\sum_c T_c}\right) \Big/ \left(1 + 3\frac{\overline{T}}{\sum_c T_c}\right); \quad \overline{T} = \frac{\sum_c T_c^2}{\sum_c T_c}. \tag{5}$$

This formula fulfils the Agasi-Weidenmüller limit [15], which predicts $W_a = 2$ for $\sum_c T_c$ going to infinity, even when $T_a \ll 1$. The simplest way of solving equation (3) is by iteration method. Making use of the fact that $V_a(\sum_c V_c)^{-1} \cong T_a(\sum_c T_c)^{-1}$ we obtain

$$V_a^{(1)} = T_a\left[1 + \frac{T_a}{\sum_c T_c}(W_a - 1)\right]^{-1}. \tag{6}$$

Already formula (6) approaches the exact solution of equation (3), when the number of open channels does exceed 20. If not, we follow

$$V_a^{(i+1)} = T_a\left[1 + \frac{V_a^{(i)}}{\sum_c V_c^{(i)}}(W_a - 1)\right]^{-1}. \tag{7}$$

The transmission coefficients for radiative transitions are related to the strength function $f_\gamma(E_\gamma)$,

$$T_{\gamma_c} = 2\pi f_{\gamma_c}(E_{\gamma_c}) E_{\gamma_c}^{2L+1}. \tag{8}$$

Formulae (2) to (8) were applied in the present calculations, which have been conducted with use of the EMPIRE code [16]. A complete γ-ray cascade, consisting of transitions between and from the continuum states, as well as of transitions between the discrete levels, was accounted for in the calculations. The neutron, proton and radiative channels were assumed to be relevant for a comparison of the results of calculation with experiment. The population of excited levels with known spins and parities was treated accurately, and for excitation energies surpassing the highest known level the level density by Cameron and Gilbert [17] was used to describe the level spectrum.

The parametrisation of the calculation follows the method outlined by Reffo [18]. We have analysed all the experimental information relevant to the determination of the radiative width and level densities for all nuclei participating in the investigated reactions. Where resonance schemes were available the staircase analysis was conducted and the resulting average level spacings were used for determination of the level density parame-

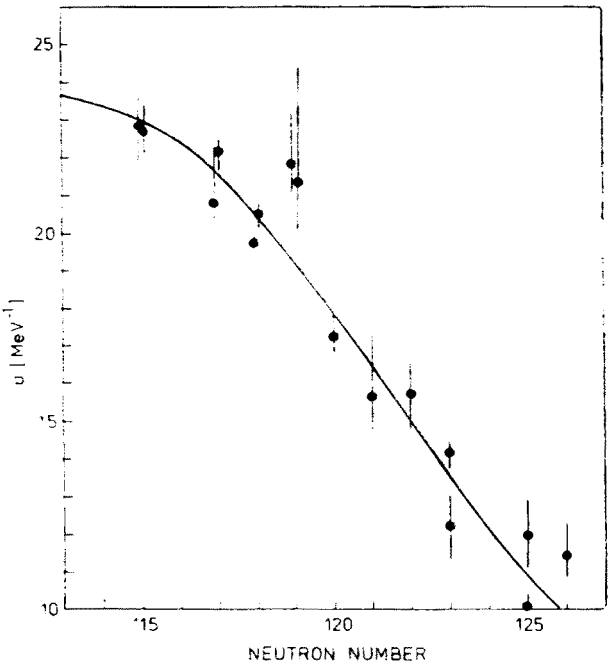

Fig. 2. Overall systematic trend of the level density parameter a (MeV $^{-1}$) versus neutron number

ter a [19]. The overall systematics (Fig. 2), including the results of our analysis, was consequently assumed to hold for all isotopes, for which no resonance schemes were known. At transitional energies, lying between the known low excited levels and the densely spaced resonance levels, the low and high energy level density laws were kept tangent. Since the matching point U_x follows too a well defined systematic trend [18], the values of U_x obtained in our analysis were checked against the overall systematics. The U_x values were interpolated in cases where the low lying levels were not adequate enough. The pairing energies Δ were taken from Cameron and Gilbert [17]. Once a, U_x and Δ have been fixed the remaining level density parameters, namely the nuclear temperature T and E_0, which defines the energy dependence of the constant temperature, low energy formula, could be calculated.

The spin cut-off parameter σ^2 was evaluated either from the average taken over angular momentum projections of the shell model single particle orbits close to the Fermi-level [18],

$$\sigma^2 = 0.24 g A^{2/3} \sqrt{\frac{U}{a}}, \tag{9}$$

or, at excitation energies below U_x, from the spins of individual excited levels

$$\sigma^2 = \frac{1}{2N} \sum_{i=1}^{N} (I_i + \tfrac{1}{2})^2, \tag{10}$$

where N is the number of known excited levels with the ground state excluded.

No parity distribution analysis was possible because of poor knowledge of states with unnatural parity in the isotopes of interest. Thus an equal distribution of levels between the two parities had to be assumed. This assumption may affect the radiative width calculation through the electromagnetic selection rules.

The radiative strength function was calculated according to the Axel prescription [20] with the giant dipole resonance parameters taken from photoreaction data. For E2 and M1 transitions the Weisskopf strengths were modified appropriately in order to reproduce the experimental results.

The optical model transmission coefficients for neutrons were calculated with the potential of Moldauer [21] and for protons the Becchetti and Greenlees potential was used [22].

Comparison of the results of calculations with the present experiment and with the data obtained by Lindner et al. [10], shown in Fig. 2, displays some deviations between the two data sets and/or the calculations. The giant dipole resonance parameters taken from global systematics provide radiative widths, at thermal energies, about 80 MeV in accordance with experiment [24]. The resulting cross sections are satisfactory for ^{191}Ir (solid line) but low for ^{193}Ir (dashed line). Alternatively we have extrapolated, for ^{194}Ir, the giant resonance strength obtained from photoneutron yields measured for individual irydium isotopes [23]. This brought the calculation into a good agreement with experiment at neutron energies around 1 MeV (solid line), however the corresponding radiative width, at thermal energy, turned out to be 150 MeV, which is high with respect to the measured value. Besides at low neutron energies the solid lines exceed the experimental data by about 30%. It is our experience that these inconsistencies cannot be removed without breaking the consequent parametrisation of the calculations. One can of course resort to the uncertainties of the parameter systematics in order to avoid the difficulty but this is not very conclusive [19]. It seems however that there is no call for another reaction mechanism and that the compound nucleus concept explains the gross behaviour of the capture cross sections in the neutron energy range investigated. This conclusion seems to be valid at even higher neutron energies [25].

REFERENCES

[1] G. Magnusson, I. Bergqvist, *Nucl. Technol.* **34**, 114 (1977).
[2] G. Magnusson, P. Andersson, I. Bergqvist, *Phys. Scr.* **21**, 21 (1980).
[3] I. Bergqvist, M. Potokar, Proc. 3d Int. Symp. on Neutron Capture, BNL, Upton-New York 1978.
[4] A. Lindholm, L. Nilsson, M. Ahmad, M. Anwar, I. Bergqvist, S. Joly, *Nucl. Phys.* **A339**, 205 (1980).
[5] H. M. Hofmann, J. Richert, J. W. Tepel, H. A. Weidenmüller, *Ann. Phys.* USA **90**, 403 (1975).
[6] H. Gruppelaar, G. Reffo, *Nucl. Sci. Eng.* **62**, 756 (1977).
[7] L. Zemło, Institute of Nuclear Research report INR-1164/I/PL/B 1973.
[8] M. Herman, Institute for Nuclear Studies, unpublished.
[9] N. D. Dudey, R. Kennerley, BNL-NCS 50446 (1975), ENDF/B-III MAT. 6410.
[10] M. Lindner, R. J. Nagle, J. H. Landrum, *Nucl. Sci. Eng.* **59**, 381 (1976).
[11] V. A. Tolstikov, V. P. Koroleva, V. E. Kolesov, A. G. Dovbienko, *Atomnaja Energia* **23**, 151 (1967).

[12] J. W. Tepel, H. M. Hofmann, H. A. Weidenmüller, *Phys. Lett.* **49B**, 1 (1974).
[13] M. Herman, A. Marcinkowski, *Nucl. Phys.* **A357**, 1 (1981).
[14] H. M. Hofmann, T. Mertelmeier, M. Herman, J. W. Tepel, *Z. Phys.* **A297**, 153 (1980).
[15] D. Agassi, H. A. Weidenmüller, G. Mantzouranis, *Phys. Rep.* **22**, 145 (1975).
[16] M. Herman, A. Marcinkowski, K. Stankiewicz, *Comp. Phys. Commun.* **33**, 373 (1984).
[17] A. G. W. Cameron, G. Gilbert, *Can. J. Phys.* **43**, 1446 (1965).
[18] G. Reffo, CNEN report RT/FI/78/11, Bologna 1978.
[19] F. Fabbri, G. Reffo, M. Herman, A. Marcinkowski, Proc. 2nd Int. Symp. on Neutron Induced Reactions, Smolenice 1979.
[20] P. Axel, *Phys. Rev.* **126**, 671 (1962).
[21] P. A. Moldauer, *Nucl. Phys.* **47**, 65 (1963).
[22] F. D. Becchetti, G. N. Greenlees, *Phys. Rev.* **182**, 1190 (1969).
[23] A. M. Goryachev, G. N. Zalesnyi, *Sov. J. Nucl. Phys.* **27**, 779 (1978).
[24] S. F. Mughabghab, D. I. Garber, BNL-325, Vol. 1, 1973.
[25] P. Andersson, R. Zorro, I. Bergqvist, University of Lund report LUNFD6/NFFR-3043/1-26/1982.